Journal of Catalysis 279 (2011) 361–365

Contents lists available at ScienceDirect

Journal of Catalysis

journal homepage: www.elsevier.com/locate/jcat

A novel Au&Pd/Fe(OH)$_x$ catalyst for CO + H$_2$ co-oxidations at low temperatures

Botao Qiao [a,b], Aiqin Wang [a], Masashi Takahashi [c], Yanjie Zhang [a], Junhu Wang [a], Youquan Deng [b,*], Tao Zhang [a,*]

[a] State Key Laboratory of Catalysis, Dalian Institute of Chemical Physics, Chinese Academy of Sciences, Dalian 116023, China
[b] Centre for Green Chemistry and Catalysis, Lanzhou Institute of Chemical Physics, Chinese Academy of Sciences, Lanzhou 730000, China
[c] Department of Chemistry, Faculty of Science, Toho University, Miyama, Funabashi, Chiba 274-8510, Japan

ARTICLE INFO

Article history:
Received 30 November 2010
Revised 9 February 2011
Accepted 10 February 2011
Available online 22 March 2011

Keywords:
Gold
Palladium
Bimetal
Separate active sites
Co-oxidation

ABSTRACT

A novel Au&Pd/Fe(OH)$_x$ catalyst with separate Au and Pd active sites was designed and synthesized. It was found for the first time that total conversion of CO + H$_2$ could be achieved at room temperature over this catalyst. The separate Au and Pd sites in Au&Pd/Fe(OH)$_x$ catalyst were confirmed by the XPS, XRD, ^{197}Au Mössbauer characterizations and the activity measurements, although a small amount of Au–Pd alloy formed after the catalyst was calcined at 500 °C.

1. Introduction

Catalytic oxidations of CO, H$_2$ and CO + H$_2$ over supported noble metals such as Au, Pd and Pt catalysts at lower temperature have attracted considerable attention and have been studied extensively because of their great importance for both practical applications and fundamental research of catalysis sciences [1–7]. For example, one of the important applications of CO + H$_2$ co-oxidation is CO-tolerant hydrogen oxidation in fuel cell [8]. It is well known that, at ambient temperature, supported Pt and Pd are the most effective catalysts for H$_2$ oxidation [9,10], while supported Au catalysts are intrinsically more active for CO oxidation [11–13]. For co-oxidation of CO + H$_2$, it has been generally observed that the oxidation of H$_2$ was strongly inhibited by the presence of CO, which resulted in the retarded activity for co-oxidations of CO + H$_2$ over the traditional Pd, Au, Pt, Pd–Au and Pt–Au catalysts [1,8,14,15]. Recently, Eichhorn's group developed several bimetal nanoparticles with various structures which were highly effective for the co-oxidation of CO + H$_2$ [16,17]. They found Ru@Pt particles with core-shell structure were particularly active for co-oxidation of CO + H$_2$ with lower CO concentration (1000 ppm). However, the activity decreased with the increase in CO concentration [17]. Therefore, simultaneous oxidation of H$_2$ + CO at low temperatures, especially with relatively high CO concentration (for example 1 vol%), still remains to be a challenging subject.

It has now been recognized that the preparation methods played a key role in determining the chemical and physical properties of supported metal catalysts and, ultimately, their performance in catalytic reactions. In our previous study, we found that ferric hydroxide-supported Au catalysts prepared by a coprecipitation method without calcination possessed high activity for the selective oxidation of CO in the presence of H$_2$ and was less affected by the presence of H$_2$ [18,19]. This offered the hint to design a Au–Pd (Au–Pt) bimetallic catalyst with separate active sites to resolve the challenging subject mentioned above, viz., CO was oxidized over Au active sites, while H$_2$ was oxidized over Pd (Pt) active sites.

The possible bimetallic architectures known currently are shown in Scheme S1. The former four architectures are often developed to alter the electronic or geometric structure and thus to change their catalytic performance (activity and/or selectivity) [20–24]. However, along with these changes, the intrinsic properties of the individual metals usually changed. Therefore, to achieve the purpose of CO and H$_2$ oxidation over Au and Pd (Pt) sites respectively, the bimetallic catalysts need to be designed in the form of mixture of monoparticles, which, to the best of our knowledge, have not been reported previously. In this work, an attempt was made to prepare ferric hydroxide-supported Au and Pd catalyst with coprecipitation without any further calcination. Since calcination was omitted, possible interaction of Au and Pd may be greatly reduced and separate Au and Pd active sites may be

* Corresponding authors. Fax: +86 931 4968116 (Y. Deng), fax: +86 411 84685940 (T. Zhang).
E-mail addresses: ydeng@lzb.ac.cn (Y. Deng), taozhang@dicp.ac.cn (T. Zhang).

0021-9517/$ - see front matter © 2011 Elsevier Inc. All rights reserved.
doi:10.1016/j.jcat.2011.02.005

established, on which CO and H_2 oxidation proceeds separately to achieve the purpose of co-oxidation of CO + H_2 at lower temperatures. In addition, coprecipitation method often leads to highly dispersed metal particles and makes the particles embedded or partially embedded in the supports [25]. The former will reduce the chance of interaction between Au and Pd, while the latter will result in a strong interaction between metal and support which will restrain the migration of metal and subsequently the formation of Au–Pd alloy.

2. Experiment

2.1. Catalyst preparation

The Au/Fe(OH)$_x$, Pd/Fe(OH)$_x$ and Au&Pd/Fe(OH)$_x$ (& represents Au and Pd particles dispersed separately on the carrier) catalysts were prepared by coprecipitation technique according to the previous work [19]. Under stirring, an aqueous mixture of $Fe(NO_3)_3$ and $HAuCl_4$ (or $(NH_4)_2PdCl_4$ or $HAuCl_4$ + $(NH_4)_2PdCl_4$) was added dropwise to Na_2CO_3 solution, and the final pH of the solution was controlled to ca. 8. The resultant precipitate was filtered and washed with distilled water for several times to remove chloride ions, then dried at 60 °C for 5 h. For comparison, these catalysts were further calcined in air at 500 °C and were denoted as Au/Fe_2O_3, Pd/Fe_2O_3 and Au–Pd/Fe_2O_3.

2.2. Measurements of catalytic activities

Catalytic activity measurements were conducted using a fixed microreactor charged with 60 mg of catalyst (60–80 mesh). The temperature of the catalyst bed was tested as reaction temperature by inserting the thermocouple into the catalyst. Then, the gas mixture containing 1 vol% CO, 1 vol% H_2, 4 vol% O_2 balanced with Ar (denoted as CO + H_2), or 1 vol% CO (1 vol% H_2) balanced with air was fed into the reactor with a space velocity of 20,000 ml g_{cat}^{-1} h^{-1}. The concentrations of H_2, CO and O_2 were online analyzed with an Agilent 1790T gas chromatograph equipped with a micro-thermal conductivity detector and a molecular sieve 5A column, using Argon as carrier gas. The catalytic activities were evaluated with the lowest temperature of total conversion (LTT) of the reaction gas.

2.3. Characterization techniques

The loadings of Au and Pd were determined on a 3520 ICP AES instrument (ARL Co., USA). X-ray diffraction (XRD) patterns were recorded on a PW3040/60 X' Pert Pro Super (PANalytical) diffractometer equipped with a Cu Kα radiation source (λ = 0.15432 nm), operating at 40 kV and 40 mA. BET surface area was measured on a Micromeritics ASAP 2010 instrument. Au/Fe(OH)$_x$, Pd/Fe(OH)$_x$ and Au&Pd/Fe(OH)$_x$ samples were outgassed to 0.1 Pa at 50 °C. The surface composition and the chemical state of catalysts were examined by XPS using a VG ESCALAB 210 instrument. Transmission electron microscopic (TEM) and high-resolution electron microscopic investigations were carried out using a JEOL JEM-2100 Electron Microscope. The ^{197}Au Mössbauer spectra were measured at 12 K using a ^{197}Pt/Pt source (224 GBq) on a Mössbauer spectrometer from Wissel, comprising MDU-1200, DFG-1200, MVT-1200 and MVC-1200 [26].

3. Results and discussion

The results in Table S1 showed that after calcination, the surface area of ferric hydroxide-supported Au and/or Pd decreased greatly, while the Au and/or Pd loadings increased slightly. These should be related to the loss of water and/or the transformation of ferric hydroxide into oxide during heat treatment process. XPS analysis indicated that the surface chemical states of Au and Pd existed as oxidized or partially oxidized states (B.E. of Au4f$_{7/2}$ = 84.1 and 84.3 eV, and B.E. of Pd3d$_{5/2}$ = 338.0 and 338.1 eV) over ferric hydroxide-supported Au, Pd and Au&Pd samples, Table S1. Upon calcination at 500 °C, Au oxide decomposed to form metallic Au completely (B.E. Au4f$_{7/2}$ = 83.5–83.6 eV), while Pd remained as oxidized state. It should be noted that the B.E. of Pd3d$_{5/2}$ over Au–Pd/Fe_2O_3 was lower than that over Pd/Fe_2O_3, suggesting the partial formation of Au–Pd alloy, which was well consistent with the previous report [27]. It can be seen from the atomic ratio of Au(Pd)/Fe (Table S1) that Au and/or Pd were enriched on the surface of all samples after being calcined at 500 °C. This enrichment clearly suggested that the migration of Au and Pd occurred certainly upon calcination, which would arouse the aggregation and the formation of alloy, especially considering that Au and Pd are miscible. XRD analyses (Fig. S1) showed that, as expected, the structures of ferric hydroxide-supported Au, Pd (similar to that of Au&Pd and not given here) and Au&Pd catalysts were amorphous, and no Au or Pd diffractive peak could be observed. After calcination at 500 °C, distinct crystallite of α-Fe_2O_3 was formed, while Au and Pd (or PdO) crystallite were still unobserved over 1.2 wt% Au/Fe_2O_3 and 1.8 wt% Pd/Fe_2O_3, suggesting they were highly dispersed. Over 1.2/1.8 wt% Au–Pd/Fe_2O_3 catalyst, however, a very faint diffractive peak of PdO(1 0 1) and a visible diffractive peak of Au(1 1 1) were observed, indicating both Au and Pd were slightly aggregated during calcination. It should be noted that the Au(1 1 1) peak (38.6°) slightly shifted to higher angle and located between Au(1 1 1) and Pd(1 1 1) positions, suggesting Au-rich Au_xPd_y alloy phase was partially formed during calcination [27], which well accorded with the XPS results. Based on the XPS and XRD results, it can be conjectured that Au and Pd species might be separate over Au&Pd/Fe(OH)$_x$ catalyst.

To clearly demonstrate the separate existence of Au and Pd species, the ^{197}Au Mössbauer spectra of these gold-containing catalysts were measured (Fig. 1), and the corresponding parameters were summarized in Table S2. It should be noted that the Au loadings of these catalysts were as high as 5 wt% to obtain better spectra, and accordingly, the Pd loadings were about 5 wt% to keep a close ratio of Au/Pd to that of 1.1/1.6 wt% Au&Pd/Fe(OH)$_x$ catalysts. The spectra of Au/Fe(OH)$_x$ and Au&Pd/Fe(OH)$_x$ resembled each other and consisted of two Au components; one was metallic gold peaked at -1.22 mm s^{-1} and the other had a positive isomer shift (*IS*) with a small quadrupole splitting (*QS*). The relation between the *IS* and *QS* value for the latter component indicated that the gold atom was in oxidation state. Judging from the preparation method of these samples, the sites can be assigned to hydrated gold(III) oxyhydroxide, AuOOH·*x*H_2O [28–30]. Our parameters of the second component (*IS* = 1.29, *QS* = 1.75 mm s^{-1}) were very close to those of Wagner et al. (*IS* = 1.37, *QS* = 1.75 mm s^{-1} for a sample containing 1.17 wt% Au, for example) [28]. Wagner et al., however, showed that the nature of this gold(III) oxyhydroxide phase depended on the preparation conditions sensitively and was difficult to specify in detail. So, it is obvious that the Au^{3+} (and Pd^{2+}, if present) ions were coprecipitated with iron(III) ions as hydrated oxyhydroxide though its nature remained undefined.

The Mössbauer spectra of Au/Fe_2O_3 and Au–Pd/Fe_2O_3 were also similar to each other. Au/Fe_2O_3 showed a symmetric absorption with a narrow linewidth. The Mössbauer parameters for this compound (*IS* = -1.18, *QS* = 0, Γ_{exp} = 2.44 mm s^{-1}) clearly corresponded to metallic gold, indicating that the gold(III) oxyhydroxide species converted to metallic gold during the calcination at 500 °C. Finch et al. also reported the same results under a similar condition [29]. The spectrum of Au–Pd/Fe_2O_3 consisted of two gold species though it looked like a single absorption peak. One was assigned

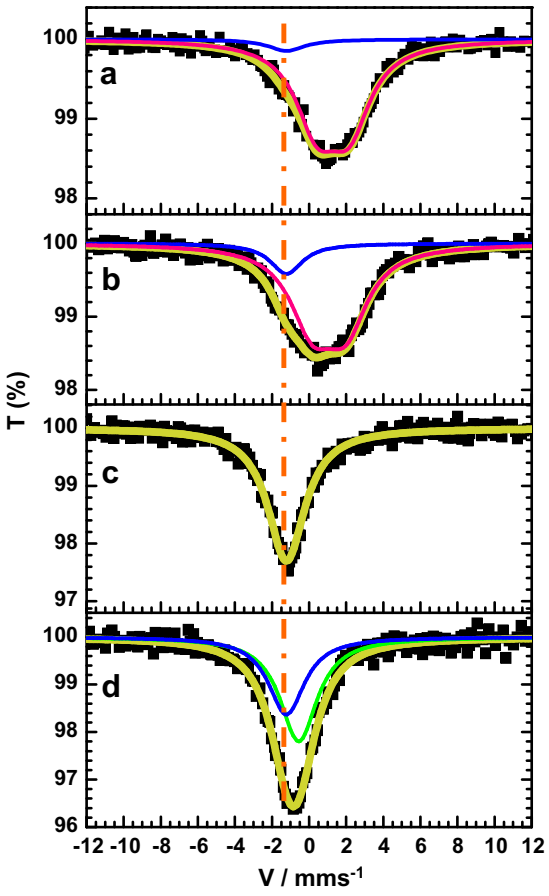

Fig. 1. ^{197}Au Mössbauer spectra for 5 wt% Au/Fe(OH)$_x$ (a), 5/5 wt% Au&Pd/Fe(OH)$_x$ (b), 5 wt% Au/Fe_2O_3 (c) and 5/5 wt% Au&Pd/Fe_2O_3 (d) catalysts measured at 12 K.

to metallic gold with an IS of −1.22 mm s^{-1}. The other with slightly positive IS of −0.56 mm s^{-1} could be assigned to Au–Pd alloy particles formed on Fe_2O_3 nanoparticles. The ^{197}Au Mössbauer spectra of Au–Pd alloys had been studied and a nearly linear relation between IS of ^{197}Au and gold content had been observed previously [31,32]. The IS value increased from −1.2 mm s^{-1} for pure gold to +1.0 mm s^{-1} for $Au_{0.015}Pd_{0.985}$ with a slight negative curvature around $Au_{0.50}Pd_{0.50}$ [32]. Lam and Boudart proved that this relation was also tenable for small Au–Pd particles on silica gel [33]. Hence, we can estimate that the gold content in our Au_xPd_y alloy in Au–Pd/Fe_2O_3 samples was 67 ± 2 atomic% according to the Longworth's results ($x_{Au} = 0.421 - 0.42IS + 0.03IS^2 - 0.02IS^3$), which was well consistent with the XRD results.

TEM observation (Fig. S2) showed that no structural changes between pure Fe(OH)$_x$ and ferric hydroxide-supported Au&Pd could be discriminated (images of Au/Fe(OH)$_x$ and Pd/Fe(OH)$_x$ were similar to those of Fe(OH)$_x$ and Au&Pd/Fe(OH)$_x$ and therefore not given). The invisibility of Au and/or Pd particles suggested that Au and Pd species were highly dispersed on/into Fe(OH)$_x$ or too small to be distinguished from the speckle contrast exhibited by the support. After being calcined at 500 °C, Au particles with 2–5 nm in size were clearly visible and the aggregation of supports was also observed over Au/Fe_2O_3, while Pd or PdO particles were still invisible over Pd/Fe_2O_3. For Au–Pd/Fe_2O_3 catalyst, metal particles (most probably Au) with 3–10 nm were formed. The results of XRD and TEM showed that Au species were prone to aggregation and PdO species alone were quite stable. The PdO species, however, would be promoted to aggregation in the presence of Au with calcination at elevated temperatures, indicating that the strong interaction between Au and Pd might occur.

Catalytic activity measurements showed that (Table S1), for individual CO or H_2 oxidation, Au/Fe(OH)$_x$ catalyst (entry 1) was highly active for CO oxidation but much less active for H_2 oxidation. Pd/Fe(OH)$_x$ catalyst (entry 2), as expected, was highly active for H_2 oxidation (LTT < 10 °C) but relatively less active for CO oxidation (LTT was 55 °C). Au&Pd/Fe(OH)$_x$ catalyst (entry 3), however, was highly active for both reactions (LTTs were 12 °C for CO oxidation and <10 °C for H_2 oxidation), suggesting that CO oxidation over Au sites and H_2 oxidation over Pd sites might occur individually. It also suggested that separate active sites of Au and Pd existed in Au&Pd/Fe(OH)$_x$ catalyst. As for co-oxidation of CO + H_2 over various catalysts, the catalytic behaviors changed markedly; over Au/Fe(OH)$_x$ catalyst, CO oxidation was slightly inhibited by the presence of H_2, while H_2 oxidation was still much poor, thus resulting in the total conversion of CO + H_2 occurring at as high as 125 °C. Over Pd/Fe(OH)$_x$ catalyst, the CO oxidation was slightly promoted by the presence of H_2, while the H_2 oxidation was seriously inhibited by the presence of CO, leading to the total conversion of CO + H_2 accomplished at 52 °C. As to Au&Pd/Fe(OH)$_x$ catalyst, even though both CO and H_2 oxidation were slightly inhibited by each other and only after CO was almost removed could the H_2 oxidation start, relative lower LTTs of 16 and 17 °C for CO and H_2 oxidations can be achieved, which, to the best of our knowledge, is the highest activity so far for co-oxidation of CO + H_2 over various catalysts. For comparison, the catalysts of Au/Fe_2O_3, Pd/Fe_2O_3 and Au–Pd/Fe_2O_3, which resulted from calcination of the corresponding Fe(OH)$_x$-supported catalysts at 500 °C, were also tested, Table S1. Probably due to the high calcination temperature and the lower Au loading, Au/Fe_2O_3 catalyst exhibited an unexpected lower activity for CO and H_2 oxidations. Pd/Fe_2O_3 and Au–Pd/Fe_2O_3 catalysts were also less active for CO oxidation compared with Pd/Fe(OH)$_x$ and Au&Pd/Fe(OH)$_x$ catalysts, while they were still active for H_2 oxidation and the LTTs were all <10 °C. For CO + H_2 co-oxidations, it can be prospective that all the catalysts were inactive at lower temperature due to the lower activity for CO.

To obtain the details of the mutual effect of CO and H_2 during the CO + H_2 co-oxidation, the curves of temperature-programmed co-oxidation of CO + H_2 over different catalysts are shown in Fig. 2. Au/Fe(OH)$_x$ catalyst had a better performance for selective oxidation of CO in the presence of H_2, and H_2 oxidation did not start even after CO was totally removed, well consistent with our previous report [18]. Therefore, it cannot be good catalyst for

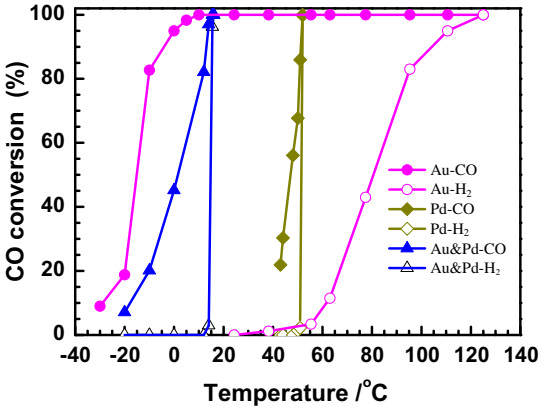

Fig. 2. Curves of CO (solid symbol) and H_2 conversion (open symbol) for CO + H_2 co-oxidation as a function of reaction temperature over various catalysts: circle, 1.1 wt% Au/Fe(OH)$_x$; diamond, 1.6 wt% Pd/Fe(OH)$_x$; triangle, 1.1/1.6 wt% Au&Pd/Fe(OH)$_x$.

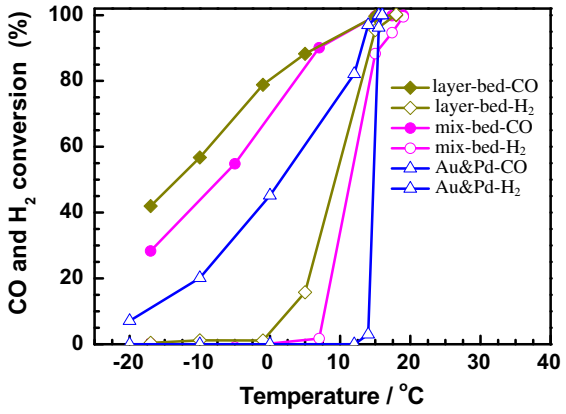

Fig. 3. Curves of CO (solid symbol) and H_2 conversion (open symbol) for CO + H_2 co-oxidation as a function of reaction temperature over various catalyst beds: triangle, 1.1 wt% Au/Fe(OH)$_x$ + 1.6 wt% Pd/Fe(OH)$_x$ with a physical mixture bed (10,000 ml g_{cat}^{-1} h^{-1}); diamond, 1.1 wt% Au/Fe(OH)$_x$ + 1.6 wt% Pd/Fe(OH)$_x$ with two-layer bed (10,000 ml g_{cat}^{-1} h^{-1}); circle, 1.1/1.6 wt% Au&Pd/Fe(OH)$_x$ alone (20,000 ml g_{cat}^{-1} h^{-1}).

CO + H_2 co-oxidation due to its lower activity for H_2 oxidation. Over Pd/Fe(OH)$_x$ catalyst, CO conversion was gradually increased with the increase in reaction temperature, while H_2 oxidation could not start due to the inhibiting effect of CO. When reaction temperature was higher than 50 °C, at which most of CO was oxidized to CO_2, the H_2 oxidation started and accomplished quickly. Therefore, the total conversion of CO + H_2 co-oxidation was achieved at about 52 °C. Based on this result, one can infer reasonably that the activity for CO + H_2 co-oxidation over Pd/Fe(OH)$_x$ catalyst or other supported Pd catalysts could be increased as long as the activity for CO oxidation was increased, since the activity for H_2 oxidation was generally high enough over supported Pd catalysts. As to Au&Pd/Fe(OH)$_x$ catalyst, the process for CO + H_2 co-oxidation was similar to that over Pd/Fe(OH)$_x$ except that the CO oxidation occurred at Au sites. It can be seen that although the activity for CO oxidation over Au&Pd/Fe(OH)$_x$ was slightly lower than that over Au/Fe(OH)$_x$, it was much higher than that over Pd/Fe(OH)$_x$ catalyst (LTT was 16 °C, at which CO oxidation had not started over Pd/Fe(OH)$_x$), indicating that CO oxidation occurred at Au sites. Similarly, the activity for H_2 oxidation over Au&Pd/Fe(OH)$_x$ was much higher than that over Au/Fe(OH)$_x$ (LTT was 17 °C, at which H_2 oxidation had not initiated over Au/Fe(OH)$_x$), indicating that H_2 oxidation occurred at Pd sites. The curves clearly suggested that CO + H_2 co-oxidation took place separately over Au&Pd/Fe(OH)$_x$, *i.e.* CO oxidation occurred firstly at Au sites and H_2 oxidation subsequently on Pd sites, resulting in the CO + H_2 co-oxidation at a low temperature of 17 °C.

To further prove the separate active sites of Au and Pd in Au&Pd/Fe(OH)$_x$ catalyst, a control experiment for CO + H_2 co-oxidation was performed with a physical mixture (denoted as mix-bed) and a two-layer bed (denoted as layer bed) of Au/Fe(OH)$_x$ + Pd/Fe(OH)$_x$ catalysts. The details of the test condition were described in supporting information. The results presented in Fig. 3 showed that the LTTs for CO and H_2 co-oxidation over the two types of catalyst beds were essentially the same as that over Au&Pd/Fe(OH)$_x$ catalyst although the activities were slightly different at lower temperature. Although the higher activity of the layer-bed catalyst system at lower temperature (e.g. <5 °C) showed that the efficiency of noble metal was the highest among the three catalyst systems, it clearly indicates that the Au and Pd sites in Au&Pd/Fe(OH)$_x$ catalyst are isolated. In addition, compared with the mix-bed and layer-bed systems, our Au&Pd/Fe(OH)$_x$ catalyst provided a more cost-efficient candidate for CO + H_2 co-oxidation by combining two similar preparation processes into one, which is time and energy saving.

4. Conclusion

In conclusion, a novel Au&Pd/Fe(OH)$_x$ catalyst with separate Au and Pd active sites was designed and successfully prepared, and the structure was confirmed by the XRD, XPS, TEM, ^{197}Au Mossbauer spectra characterizations as well as activity measurements. Over this catalyst, the CO oxidation occurred on Au active sites, while the H_2 oxidation occurred on Pd active sites, thus the co-oxidation of CO + H_2 was realized over one catalyst at ambient temperature. Although the same function can be realized over a mixture bed or a two-layer bed constituting two different catalysts (Au/Fe(OH)$_x$ and Pd/Fe(OH)$_x$), our Au&Pd/Fe(OH)$_x$ catalyst which combines two separate active sites in one catalyst provides a more cost-efficient candidate for CO + H_2 co-oxidation. It is also a good example in fundamental research that two different metal species co-exist, but not interact with each other, on one catalyst.

Acknowledgments

This work was financially supported by the National Natural Science Foundation of China (No. 20773146) and China Postdoctoral Science Foundation (20080441104). The Mössbauer spectroscopic study was supported in part by the Inter-University Programs for the Joint Use of JAEA Facilities. We would like to thank Ms L. Gao for XPS investigation, Ms Q. Wu for the metal loading analysis, Ms L. He for XRD measurements, and Ms J. Li for measurements of BET adsorption.

Appendix A. Supplementary data

Supplementary data associated with this article can be found, in the online version, at doi:10.1016/j.jcat.2011.02.005.

References

[1] J.R. Stetter, K.F. Blurton, Ind. Eng. Chem. Prod. Res. Dev. 19 (1980) 214.
[2] M. Haruta, N. Yamada, T. Kobayashi, S. Iijima, J. Catal. 115 (1989) 301.
[3] B.N. Racine, M.J. Sally, B. Wade, R.K. Herz, J. Catal. 127 (1991) 307.
[4] M. Valden, X. Lai, D.W. Goodman, Science 281 (1998) 1647.
[5] M.M. Schubert, S. Hackenberg, A.C. van Veen, M. Muhler, V. Plzak, R.J. Behm, J. Catal. 197 (2001) 113.
[6] J. Hoffmann, S. Schauermann, J. Hartmann, V.P. Zhdanov, B. Kasemo, J. Libuda, H.J. Freund, Chem. Phys. Lett. 354 (2002) 403.
[7] A.A. Herzing, C.J. Kiely, A.F. Carley, P. Landon, G.J. Hutchings, Science 321 (2008) 1331.
[8] T.J. Schmidt, Z. Jusys, H.A. Gasteiger, R.J. Behm, U. Endruschat, H. Boennemann, J. Electroanal. Chem. 501 (2001) 132.
[9] F.V. Hanson, M. Boudart, J. Catal. 53 (1978) 56.
[10] M.G. Jones, T.G. Nevell, J. Catal. 122 (1990) 219.
[11] M. Haruta, Catal. Today 36 (1997) 153.
[12] G.C. Bond, D.T. Thompson, Catal. Rev. Sci. Eng. 41 (1999) 319.
[13] G.J. Hutchings, Catal. Today 100 (2005) 55.
[14] S. Miao, Y. Deng, Chin. J. Catal. 22 (2001) 461.
[15] P. Liu, A. Logadottir, J.K. Norskov, Electrochim. Acta 48 (2003) 3731.
[16] S. Zhou, K. McIlwrath, G. Jackson, B. Eichhorn, J. Am. Chem. Soc. 128 (2006) 1780.
[17] S. Alayoglu, A.U. Nilekar, M. Mavrikakis, B. Eichhorn, Nat. Mater. 7 (2008) 333.
[18] B. Qiao, Y. Deng, Chem. Commun. (2003) 2192.
[19] B. Qiao, J. Zhang, L. Liu, Y. Deng, Appl. Catal. A 340 (2008) 220.
[20] M. Chen, D. Kumar, C.-W. Yi, D.W. Goodman, Science 310 (2005) 291.
[21] J.K. Edwards, B. Solsona, P. Landon, A.F. Carley, A. Herzing, M. Watanabe, C.J. Kiely, G.J. Hutchings, J. Mater. Chem. 15 (2005) 4595.
[22] D.I. Enache, J.K. Edwards, P. Landon, B. Solsona-Espriu, A.F. Carley, A.A. Herzing, M. Watanabe, C.J. Kiely, D.W. Knight, G.J. Hutchings, Science 311 (2006) 362.
[23] G.J. Hutchings, Dalton Trans. (2008) 5523.
[24] L. Kesavan, R. Tiruvalam, M.H.A. Rahim, M.I.b. Saiman, D.I. Enache, R.L. Jenkins, N. Dimitratos, J.A. Lopez-Sanchez, S.H. Taylor, D.W. Knight, C.J. Kiely, G.J. Hutchings, Science 311 (2011) 195.
[25] A.M. Venezia, G. Pantaleo, A. Longo, G. Di Carlo, M.P. Casaletto, F.L. Liotta, G. Deganello, J. Phys. Chem. B 109 (2005) 2821.

[26] S.K. Bhargava, F. Mohr, M. Takahashi, M. Takeda, Bull. Chem. Soc. Jpn. 74 (2001) 1051.
[27] Z.H. Suo, C.Y. Ma, M.S. Jin, T. He, L.D. An, Catal. Commun. 9 (2008) 2187.
[28] F.E. Wagner, S. Galvagno, C. Milone, A.M. Visco, L. Stievano, S. Calogero, J. Chem. Soc., Faraday Trans. 93 (1997) 3403.
[29] R.M. Finch, N.A. Hodge, G.J. Hutchings, A. Meagher, Q.A. Pankhurst, M. Rafiq, H. Siddiqui, F.E. Wagner, R. Whyman, Phys. Chem. Chem. Phys. 1 (1999) 485.
[30] P. Landon, J. Ferguson, B.E. Solsona, T. Garcia, S. Al-Sayari, A.F. Carley, A.A. Herzing, C.J. Kiely, M. Makkee, J.A. Moulijn, A. Overweg, S.E. Golunski, G.J. Hutchings, J. Mater. Chem. 16 (2006) 199.
[31] L.D. Roberts, R.L. Becker, F.E. Obenshain, J.O. Thomson, Phys. Rev. 137 (1965) A895.
[32] G. Longworth, J. Phys. C: Sol. St. Phys. 3 (1970) S81.
[33] Y.L. Lam, M. Boudart, J. Catal. 50 (1977) 530.